Astron. Astrophys. 347, 235–242 (1999)

ASTRONOMY AND ASTROPHYSICS

On the relation between diffuse interstellar bands and simple molecular species⋆

J. Krełowski[1], P. Ehrenfreund[2], B.H. Foing[3], T.P. Snow[4], T. Weselak[1], S. Ó. Tuairisg[2], G.A. Galazutdinov[5], and F.A. Musaev[5]

[1] Center for Astronomy, Nicholas Copernicus University, Gagarina 11, PL-87-100 Toruń, Poland
[2] Leiden Observatory, P.O. Box 9513, 2300 RA Leiden, The Netherlands
[3] ESA Space Science Department, ESTEC/SCI-SO, 2200 AG Noordwijk, The Netherlands and IAS/CNRS, France
[4] University of Colorado, CASA, Campus Box 391, Boulder, CO 80309, USA
[5] Special Astrophysical Observatory, Nizhnij Arkhyz 357147, Russia

Received 25 January 1999 / Accepted 21 April 1999

Abstract. We present observations of the major diffuse interstellar bands (DIBs) at 5780 and 5797 Å as well as literature data and our own observations of the violet lines of CH and CH^+, in the lines of sight toward some 70 stars representing various degrees of the interstellar reddening. The correlations are shown and discussed in the context of indicators such as far-UV extinction parameters and neutral molecular abundances. The results show that the DIBs in question ($\lambda\lambda$5797 and 5780) both probably form in diffuse cloud interiors, in a related regime where CH and H_2 form. The ratio of the two DIBs correlates with CH abundance, confirming that the λ5797 carrier is favoured in enhanced molecular gas regions over the λ5780 carrier. The ratio of the two DIBs correlates poorly with CH^+ abundance. Our compilation of observational data also suggests that the DIB ratio may be equally useful as a cloud type indicator as is R_V, the ratio of total to selective extinction, and much more readily observed.

Key words: ISM: dust, extinction – ISM: molecules – infrared: ISM: lines and bands

1. Introduction

The identification of the carriers of the diffuse interstellar bands (DIBs) is one of the most fascinating puzzles in astronomy. Numerous efforts to identify the carrier have been made during the last 75 years since the discovery of the first two "stationary" and rather broad features in spectra of spectroscopic binaries: the yellow bands centered near 5780 and 5797 Å (Heger 1922). The latest surveys of DIB spectra (Jenniskens & Désert 1994, Krełowski et al. 1995, Herbig 1995, Ó Tuairisg et al. 1999) have shown more than 200 DIBs. Most of the newly discovered features are, however, very weak ones, detectable only in spectra of very high S/N ratio or very high E_{B-V}.

Such a wealth of weak features is consistent with the hypothesis of large molecules in interstellar clouds. Currently only a few candidates are known as possible carriers (see Herbig 1995 and Snow 1997 for a review). The DIBs are commonly believed to originate in complex carbon bearing molecules residing in the interstellar gas, such as polycyclic aromatic hydrocarbons (PAHs) (Salama et al. 1996), C-chains (Tulej et al. 1998) or fullerenes (Foing & Ehrenfreund 1994, 1997). This hypothesis is supported by the recent discovery of substructures inside profiles of well-known, strong DIBs (Sarre et al. 1995, Ehrenfreund & Foing 1996, Krełowski & Schmidt 1997, Kerr et al. 1998).

The lines of sight where DIBs are observed invariably also display lines of other, well–identified interstellar species such as Na I D_1 and D_2 or Ca II H and K along the sightlines toward distant, reddened OB stars. About a decade ago Krełowski & Walker (1987), Josafatsson & Snow (1987) and Krełowski & Westerlund (1988) demonstrated that the strength ratios of the diffuse bands (DIBs) may vary from cloud to cloud which proves that the abundances or physical state of DIB carriers inside individual clouds may be quite different. The most striking examples of this phenomenon are the two neighbour diffuse bands centered around 5780 and 5797 Å. Lines of sight, referred to as "sigma" clouds (because the line of sight toward σ Scorpii is the archetype), usually have a low ratio of 5797/5780. On the converse, "zeta" clouds (after ζ Ophiuchi), usually have a high ratio of 5797/5780 (Krełowski & Westerlund 1988).

During the last decade it was shown that the DIB intensity ratios vary from cloud to cloud together with the strengths (measured in relation to E_{B-V}) of spectral features of simple molecules such as CN or CH (Krełowski et al. 1992). Investigations of the features originating in simple molecules such as CH or CH^+ are attractive as they can lead to a determination of the physical conditions of the cloud which may influence the formation of the DIB carriers or protect them against possible destructive processes such as far–UV photons. It remains to be

Send offprint requests to: P. Ehrenfreund

⋆ Based on observations obtained at the Russian Special Astrophysical Observatory (SAO), Terskol Observatory (TER), Canada France Hawaii Telescope (CFHT), European Southern Observatory (ESO), Observatoire de Haute-Provence (OHP)

seen exactly what the relationship is between the DIB carriers, the dust, and simple molecular species such as CH. This paper is an attempt to explore this question. The present paper is based on the extensive data set of DIBs, CH and CH^+ observed by the authors as well as collected from the literature and checked for consistency.

2. The observational data

In selecting stars for our programme we have focussed our attention on existing data sets acquired with the aid of solid-state detectors with high resolution, in order to avoid problems of blending with stellar lines and noise resulting from low signal–to–noise. Most of the described targets are bright stars. By confining ourselves to such objects we accomplish two things: (1) we ensure that a very high signal–to–noise ratio can be achieved; and (2) we minimize confusion caused by the inclusion of multiple cloud components along the observed lines of sight. However, there are some stars such as HD 206165, HD207198, HD210839 in which the interstellar CaII lines are known to show double components of comparable intensity (Adams 1949, Munch 1957). The measurements of molecular features of CH and CH^+ as well as the major diffuse bands, 5780 and 5797 have been collected from several published papers: Allen (1994)–**Al94**; Crane et al. (1995) – **cls**; Crawford et al. (1994) – **cr94**, Crawford (1997) – **cr97**; Danks et al. (1984) – **dfl**; Federman et al. (1994) – **F94**; Gredel et al. (1991) – **gdb**, Herbig (1993) – **her**, Jenniskens et al. (1992) – **jed** and Josafatsson & Snow (1987) – **js**.

In addition to the published data we have included our own measurements from several sources: Canada–France–Hawaii Telescope **cfht**; the data reduction procedures described e.g. by Krełowski et al. (1992); McDonald Observatory **mcd**; it is the extensive set of spectra acquired with the Sandiford echelle spectrograph fed with the 2.1-m telescope; the data reduction procedures described by Krełowski & Sneden (1993a).

Other observations have been performed with the aid of the 2.03 m Bernard Lyot Telescope of the Pic du Midi Observatory **pdm**. The instrument used is the echelle spectrograph MUSICOS, fed by an optical fiber. It allows to cover in two exposures the whole visible range (3850–8750 Å). The cross–disperser expands the spectrum over the CCD chip (Tektronix 1024×1024 elements), formed into 46 orders in the "blue" range (3850–5400 Å) and into 44 orders in the "red" range (5100–8750 Å). Each resolution element is dispersed on 3 pixels. To separate the orders and correct them for the Blaze distortion we used the data reduction software developed for MUSICOS by T. Böhm (Baudrand & Böhm, 1992) and J-F. Donati. The wavelength calibration is provided by a Thorium-Argon lamp installed in the fiber setting. Also a Tungsten lamp is used to flat-field the spectra. The sensitivity of this instrument provides a S/N ratio of ∼100 in a 30 min. exposure for a 6th magnitude star, at least in the middle of each order. The edges of each order and of the whole wavelength range are more noisy.

Additional spectra considered here are acquired with the aid of the coude echelle spectrometer fed by the 2-m telescope of the observatory on top of the peak Terskol **trl** (Northern Caucasus) and by the 1-m telescope of the Special Astrophysical Observatory (SAO) of the Russian Academy of Sciences, indicated with **sao**. With the Wright Instruments CCD 1242×1152 matrix (pixel size 22.5 μm x 22.5 μm) the spectrometer covers in a single exposure the range ∼3500 Å – ∼10100 Å with the resolution R=40,000 (SAO) and 45,000 (Terskol). Our reduction of the echelle spectra was made using the DECH code (Galazutdinov 1992). This program allows flatfield division, bias/background subtraction, one–dimensional spectrum extraction from the 2–dimensional images, correction for the diffuse light, spectrum addition, excision of cosmic ray features, among the standard operations. The DECH code also allows location of a fiducial continuum, measurements of the line equivalent widths, line positions and shifts, and other measurements. The spectral range, covered in every exposure, contains strong and well–identified atomic interstellar lines: Ca II, Ca I, Na I and K I. This allowed us to determine precisely the radial velocities of the intervening interstellar clouds at a moment of any observation with a high precision.

A rather extensive set of spectra was acquired at Observatoire de Haute Provence (OHP) using the 1.93-m telescope equipped with the ELODIE spectrograph which is indicated in the tables with **ohp** (Baranne et al. 1996). ELODIE is a fiber-fed echelle spectrograph, covering the wavelength range from 3906 to 6811 Å with a resolution of ∼ 42 000 (Baranne et al. 1996). The fibres are POLYMICRO fibres with a diameter of 100 μm. The grating used is a 408×102 mm echelle grating with 31 grooves/mm and a θ=76° blaze angle. The dispersion crossing is done with two optical components, a 40° flint prism and a 8.63° crown grism with 150 grooves/mm).

3. Results

All the collected measurements of CH and CH^+ molecular features as well as those of the 5780 and 5797 DIBs are listed in Tables 1, 2 and 3. In Table 1 stars are listed which were observed using at least 3 different instruments and where the measurements coincide within 10%. In Table 2 we list targets which were observed with at least two coinciding measurements from different sources as well as targets observed from more sites but with higher discrepancies. Table 3 summarizes stars where we have less measurements. The listed equivalent widths has been measured by integrating over the whole band even if they are evidently Doppler–split (as in the case of HD183143, well known since the Herbig & Soderblom, 1982 publication). Unfortunately some of the features under consideration have not been observed (blank entries in tables). We have included in the tables only the targets for which we could find the measurements of both DIBs: 5797 and 5780 plus at least one of the molecular features: CH – 4300.3 Å or CH^+ – 4232.5 Å.

The interstellar absorption features are usually correlated to some degree. It has already been suggested (Krelowski & Walker 1987) that the strong 5780 and 5797 DIBs are not of common origin due to their strongly variable intensity ratio which must depend on the physical conditions inside the inter-

Table 1. This table lists the stellar parameters of the programme stars and measurements of the equivalent width of CH and CH^+ features as well as of the diffuse interstellar bands at 5780 and 5797 Å. Each target in this table was observed at least by three different instruments and all measurements coincide within 10%. Superscripts after the star's HD number indicate the observatory or reference codes: a:cfht, b:mcd, c:her, d:jed, e:sao, f:ohp, g:cls, h:trl, i:js, j:dfl, k:F94, l:cr94, m:cr97, n:gdb, o:pdm, p:Al94. Values from this table are averaged and appear in the figures as solid (filled) circles. Star identifications are HD numbers.

Star	SpT	V	E_{B-V}	CH^+	CH	λ5780	λ5797	Star	SpT	V	E_{B-V}	CH^+	CH	λ5780	λ5797
2905[a]	B1Iae	4.16	0.33	13.4	8.0	277	65	154445[f]				16.8	15.0	212	59
2905[b]				-	-	293	70	154445[b]				–	–	200	60
2905[c]				-	-	282	72	154445[e]				19.3	16.4	209	60
2905[d]				13.3	6.8	-	-	179406[o]	B3V	5.34	0.31	–	16.0	146	73
2905[e]				13.2	9.2	268	73	179406[a]				4.2	14.7	–	–
23180[a]	B1III	3.82	0.27	6.0	14.8	79	64	179406[b]				-	-	143	70
23180[b]				-	-	80	65	179406[c]				-	-	155	72
23180[c]				-	-	80	59	179406[f]				-	17.5	148	69
23180[f]				8.4	15.0	77	55	184915[o]	B0.5III	4.95	0.22	5.5	4.6	157	25
23180[g]				5.5	15.3	-	-	184915[a]				6.7	6.1	148	24
23180[h]				5.5	14.8	81	69	184915[b]				-	-	156	23
23180[p]				8.1	11.0	-	-	184915[c]				-	-	165	23
24398[a]	B1Iab:	2.93	0.29	2.2	17.5	88	54	184915[f]				4.9	5.7	164	23
24398[b]				-	-	98	58	184915[g]				5.0	3.7	-	-
24398[c]				-	-	94	56	184915[p]				7.6	4.7	-	-
24398[f]				2.5	15.6	98	57	190603[a]	B1.5Iae	5.62	0.73	31.3	14.3	-	-
24398[g]				2.4	16.0	-	-	190603[f]				31.5	13.4	372	89
24398[e]				2.5	16.2	97	55	190603[i]				-	-	358	112
24398[p]				2.9	15.4	-	-	190603[d]				33.2	12.2	-	-
24912[o]	O7e	4.04	0.30	22.6	9.5	-	-	190603[e]				28.0	13.7	350	83
24912[b]				-	-	196	38	190603[p]				27.1	9.5	-	-
24912[c]				-	-	192	34	198478[o]	B3Iae	4.84	0.54	34.7	19.9	319	67
24912[f]				22.8	10.7	187	37	198478[a]				33.3	18.6	285	74
24912[g]				23.6	10.8	-	-	198478[f]				33.7	18.3	315	75
24912[e]				22.6	11.7	183	37	198478[b]				-	-	301	72
144217[b]	B0.5V	2.62	0.17	-	-	157	15	198478[d]				37.0	19.0	-	-
144217[g]				4.3	2.2	-	-	206165[a]	B2Ib	4.73	0.46	15.1	19.8	193	73
144217[f]				0.0	0.0	168	15	206165[b]				-	-	197	78
144217[j]				-	1.6	-	-	206165[c]				-	-	197	87
144217[o]				5.6	2.0	-	-	206165[f]				16.8	18.0	204	80
144217[h]				4.1	2.4	157	16	206165[d]				12.4	17.7	-	-
147933[g]	B2.5V	5.02	0.43	15.8	16.9	-	-	206267[o]	O6e	5.62	0.51	11.6	20.1	210	88
147933[j]				-	16.7	-	-	206267[a]				8.9	21.5	213	84
147933[b]				-	-	201	49	206267[b]				-	-	228	94
147933[c]				-	-	219	54	206267[e]				14.0	23.0	212	100
147933[i]				-	-	218	51	207198[a]	O9IIe	5.95	0.54	16.4	29.1	237	132
147933[k]				-	15.9	-	-	207198[b]				-	-	235	135
147933[a]				-	-	194	49	207198[c]				-	-	242	139
149757[o]	O9V	2.60	0.26	22.0	19.7	69	33	207198[h]				21.3	33.2	238	140
149757[a]				22.6	16.7	69	33	207198[d]				15.6	28.7	-	-
149757[g]				20.7	19.6	-	-	207198[e]				20.1	33.4	242	147
149757[l]				21.9	15.8	-	-	210839[o]	O6Iab	5.06	0.52	12.0	23.2	-	-
149757[b]				-	-	69	29	210839[a]				13.9	23.1	239	78
149757[c]				-	-	72	31	210839[b]				-	-	247	68
149757[f]				23.7	17.0	74	30	210839[c]				-	-	246	69
149757[h]				23.5	19.1	68	29	210839[g]				12.1	16.5	-	-
149757[j]				-	17.8	-	-	210839[f]				12.5	19.3	252	69
154445[o]	B1V	5.64	0.39	20.9	17.0	203	61	210839[e]				12.2	20.0	239	72

vening clouds. The high-resolution profile of the narrow 5797 Å DIB shows a pronounced double peak structure indicative of rotational-vibrational transitions of a gas phase molecule (Sarre et al. 1995, Ehrenfreund & Foing 1996). In contrast the 5780 Å

Table 2. This table lists the stellar parameters of the programme stars and measurements of the equivalent width of CH and CH^+ features as well as of the diffuse interstellar bands at 5780 and 5797 Å. Each target was observed with at least two coinciding measurements from different sources. In this table we include also targets which were observed from more sites but with higher discrepancies. Superscripts after the star's HD number indicate the observatory or reference codes: a:cfht, b:mcd, c:her, d:jed, e:sao, f:ohp, g:cls, h:trl, i:js, j:dfl, k:F94, l:cr94, m:cr97, n:gdb, o:pdm, p:Al94. Values from this table are averaged and appear in the figures as starred points "bl" denotes blend.

Star	SpT	V	E_{B-V}	CH^+	CH	λ5780	λ5797	Star	SpT	V	E_{B-V}	CH^+	CH	λ5780	λ5797
22951[b]	B0.5V	4.97	0.26	-	-	90	32	164353[g]				4.3	3.0	-	-
22951[c]				-	-	94	36	164353[f]				8.0	7.6	129	20
22951[f]				11.0	7.8	101	36	164353[j]				-	4.1	-	-
22951[e]				9.6	10.3	90	31	164353[e]				6.7	7.4	121	23
27778[f]	B3V	6.36	0.37	7.8	24.0	74	35	167263[a]	B0.5Ib	5.95	0.22	7.6	6.9	284	74
27778[a]				-	23.4	78	33	167263[c]	/II			-	-	299	79
30614[g]	O9.5Iae	4.29	0.27	15.5	5.6	-	-	167263[j]				-	4.3	-	-
30614[i]				-	-	118	54	167264[a]	B0.5Ia	5.38	0.27	8.3	5.7	220	79
30614[f]				16.4	7.2	137	52	167264[c]	/Iab			-	-	232	87
30614[d]				18.6	1.6	-	-	167264[j]				-	4.1	-	-
30614[e]				15.6	7.0	112	47	169454[a]	B1Ia	6.63	1.09	15.2	-	458	186
34078[h]	O9Ve	5.94	0.49	44.0	54.0	170	56	169454[c]				-	-	502	192
34078[b]				-	-	186	60	169454[n]				16.0	26.2	-	-
34078[d]				52.0	42.0	-	-	169454[m]				-	25.9	-	-
34078[i]				-	-	180	65	169454[k]				-	34.7	-	-
34078[p]				44	48.3	-	-	169454[p]				12.7	26.2	-	-
41117[o]	B2Iae	4.60	0.47	15.0	13.1	338	117	183143[a]	B7Ia	6.84	1.31	48.2	34.0	751	230
41117[b]				-	-	341	116	183143[b]				-	-	753	203
41117[g]				22.4	12.9	-	-	183143[c]				-	-	774	237
41117[d]				15.0	12.0	-	-	183143[f]				49.3	36.0	792	190
143275[g]	B0.2IV	2.30	0.14	1.5	1.7	-	-	183143[n]				49.8	30.7	-	-
143275[b]				-	-	79	14	183143[d]				57	36	-	-
143275[j]				-	1.8	-	-	183143[h]				54.3	42.1	740	209
143275[o]				3.9	1.7	-	-	193237[o]	B2e	4.81	0.61	31.7	5.7	217	69
143275[e]				3.9	1.3	79	16	193237[b]				-	-	212	71
145502[f]	B2IV	4.01	0.24	5.1	5.5	187	31	193237[f]				33.5	8.4	204	72
145502[a]				-	-	167	33	194279[h]	B1.5Ia	7.01	1.20	40.7	36.1	463	139
145502[b]				-	-	175	29	194279[f]				34.0	31.0	469	144
145502[c]				-	-	182	41	199579[a]	O6Ve	5.96	0.35	14.4	15.2	123	50
145502[j]				-	4.9	-	-	199579[o]				14.3:	14.5	-	-
145502[i]				-	-	178	35	199579[f]				13.3	15.5	131	47
147165[i]	B1III	2.88	0.34	-	-	240	32	199579[b]				-	-	117	49
147165[j]				-	2.6	-	-	199579[c]				-	-	136	52
147165[b]				-	-	244	23	199579[d]				8.0	19.0	-	-
147165[f]				4.5	3.2	246	24	203064[a]	O8e	5.00	0.27	5.7	7.8	156	45
148184[g]	B2Vne	4.42	0.49	11.0	19.6	-	-	203064[o]				7.3	5.9	-	-
148184[j]				-	23.0	-	-	203064[b]				-	-	164	46
148184[b]				-	-	104	48	203064[c]				-	-	184	49
148184[c]				-	-	98	64	203064[g]				6.5	6.8	-	-
163472[o]	B2IV	5.82	0.30	8.9	11.4	218	84	208501[o]	B8Ib	5.80	0.76	–	43.8	-	–
163472[e]				9.2	9.9	215	86	208501[b]				–	-	227	97
164353[o]	B5Ib	3.97	0.10	6.5	4.1	121	23	208501[f]				bl	36.8	235	98

DIB is very broad and shows no substructure in high resolution observations. The extreme constancy of the band position of the 5780 Å DIB in the different regions of the Rho Ophiuchi cloud argues against a solid state origin of the band (Seab & Snow 1995). The DIBs show a strong dependence on the interstellar UV radiation field (Snow et al. 1995). It was observed that the 5780 Å DIB can also survive in regions of high UV flux, such as Orion (Krelowski & Sneden 1993b). If these differences in behaviour are due to ionization differences, they indicate a strong dependence of the DIB carriers on ionization (Cami et al. 1997, Sonnentrucker et al. 1997, Krelowski et al. 1998). Under this interpretation, the λ5797 carrier is easily ionized and is already largely destroyed when the λ5780 carrier reaches its maximum. Thus the behaviour of these two DIBs allows us to distinguish

Table 3. This table lists the stellar parameters of the programme stars and measurements of the equivalent width of CH and CH^+ features as well as of the diffuse interstellar bands at 5780 and 5797 Å. For those targets we have in general less than two measurements. Superscripts after the star's HD number indicate the observatory and reference codes: a:cfht, b:mcd, c:her, d:jed, e:sao, f:ohp, g:cls, h:trl, i:js, j:dfl, k:F94, l:cr94, m:cr97, n:gdb, o:pdm, p:Al94. Values from this table are averaged and appear in the figures as open circles. "un" denotes features which are too weak to be accurately measured. Star identifications are HD numbers unless otherwise stated.

Star	SpT	V	E_{B-V}	CH^+	CH	λ5780	λ5797	Star	SpT	V	E_{B-V}	CH^+	CH	λ5780	λ5797
BD+40^f	O7e	9.05	1.84	65	71	754	213	152408^j				-	4.4	-	-
4220^h				-	-	715	192	166937^g	B2III:	3.85	0.41	9.2	4.9	-	-
BD+63^f	B0II	8.46	0.94	46	32	699	258	166937^b	P			-	-	285	71
IC348 12^f	A2	10.20	0.84	34	31	319	87	170740^n	B2V	5.72	0.45	14.0	16.2	-	-
14818^h	B2Iae	6.25	0.48	17	13	295	65	170740^b				-	-	234	62
15629^f	O5e	8.42	0.72	23	17	453	99	185859^e	B0.5Iae	6.52	0.57	22.0	21.0	295	193
15570^f	O4	8.13	0.96	22.4	30.7	511	146	186745^h	B9III	6.26	0.94	29	47	512	264
24534^f	O9.5pe	6.10	0.56	un	24.5	86	54	187459^e	B0.5Ibe	6.44	0.40	17.4	18.7	239	86
24534^b				-	-	75	60	193322^a	O9V	5.82	0.40	25.1	12.6	170	72
24534^c				-	-	81	61	193322^d				28.0	-	-	-
25638^h	B0III	6.99	0.65	un	34.1	260	117	193322^d				-	-	194	71
27311^f	A0	8.0	0.50	un	15	190	74	194839^f	B0.5Iae	7.49	1.20	38	32.5	539	116
36861^f	O8III	3.3	0.06	un	2.0	44	18	209744^f	B1V	6.70	0.47	9.0	18.0	208	84
40111^o	B0.5II	4.83	0.13	2.7	2.8	149	30	216200^f	B3IVe	5.93	0.25	4.8:	9.1	109	46
42087^b	B2.5Ibe	5.76	0.34	-	-	275	94	216200^b	B3IVe	5.93	0.24	-	-	102	49
42087^o				7.5	10.0	259	98	218376^o	B0.5IV	4.84	0.22	3.4:	5.2	-	-
47129^j	O8V	6.05	0.34	-	7.4	-	-	218376^b				-	-	120	38
47129^b				-	-	160	45	218376^c				-	-	131	48
47129^d				13.0	11.0	-	-	224055^h	B3Ia	7.17	0.83	-	30.5	449	144
53974^o	B0.5IV	5.39	0.29	11.7	3.9	170	51	224572^e	B1V	4.88	0.17	-	5.1	72	21
149038^a	B0Ia	4.94	0.27	25.6	8.0	214	43	228712^f	B0.5a	8.69	1.30	30.4	35.3	441	126
149038^j				-	8.6	-	-	281159^f	B5V	8.53	0.83	33.5	35.7	291	92
151804^a	O8Iab	5.22	0.35	10.5	5.4	217	42	281159^i				-	-	300	100
151804^j				-	4.2	-	-	281159^p				44	30.7	-	-
152408^a	O8If	5.77	0.43	11.5	7.8	301	43	Cyg OB28A^f	O8 Ib	9	1.61	47:	55	796	205

between clouds having low local UV fields (ζ clouds) and clouds with rather high UV flux (σ clouds), and extreme environments such as Orion. Therefore the intensity ratio of the two features can be a good and easy tracer of cloud parameters. For the high quality of measurements (rms σ uncertainties $< 1\%$ on the correlation determined by Monte Carlo simulation) we can estimate a "decorrelation bias" of 1.8 σ in the correlation (Cami et al. 1997). We found that the correlation coefficients are therefore mostly determined by real regional variations of DIBs versus reddening or photoionization differences within a region (Cami et al. 1997, Sonnentrucker et al. 1997).

Figs. 1 and 2 depict the relations between CH, CH^+ and E_{B-V} for the 70 measured targets. The relation is better for the neutral molecule, in accordance with Crawford (1989) who claimed that it relates much better to E_{B-V}. As is seen both from Figs. 1 and 2 neither CH nor CH^+ disappear when $E_{B-V} \sim 0.3$ as stated by Crawford (the points represent *measurable* features). Moreover these molecules must be present in some very tiny clouds as they are observed toward HD2905, which is characterized by a moderate reddening (E_{B-V}=0.33) and obscured by at least 4 clouds, according to Hobbs (1978). The correlation coefficients for CH/E_{B-V} and CH^+/E_{B-V} are 0.86 and 0.82, respectively.

Figs. 3 and 4 display the correlation between the strong, broad DIB at 5780 Å, the narrow and weaker diffuse band at 5797 Å respectively, and E_{B-V}. Both plots show a good correlation. A correlation coefficient of 0.89 (λ5780) and 0.80 (λ5797) was measured. One of the targets deviating from the main stream is BD +63°1964, well known to have enhanced strength of many narrow DIBs (Ehrenfreund et al. 1997). Theoretical models indicate that the line of sight toward BD +63°1964 passes through the cloud edge, where sufficient UV can excite the DIB carriers (O'Tuairisg et al. 1999).

Finally Fig. 5 presents the relation of the ratio CH/E_{B-V} to that of the 5797 to 5780 Å DIBs. Assuming the DIB ratio to be very similar in different measurements in the same target (see tables) we merged the data from different sources to average values avoiding a scatter larger than homogeneous data sets. Our sample contains very accurate measurements of different instruments for many targets which makes the results reliable. The parameters, correlated in Fig. 5, CH/E_{B-V} and the 5797/5780 DIB ratio correlate with a correlation coefficient of 0.54.

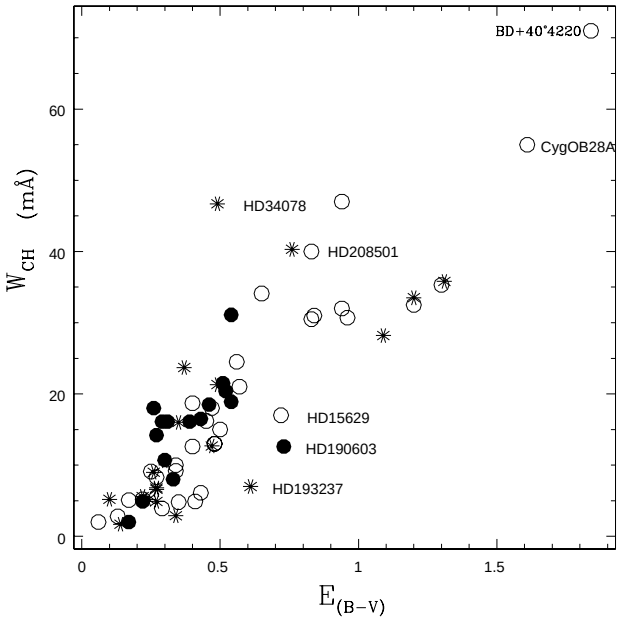

Fig. 1. This plot shows a good correlation between CH and E_{B-V} in particular at interstellar reddening between 0.2 and 0.6 for the 70 targets. The correlation coefficient is 0.86. Saturation of CH formation is observed in dense clouds at $E_{B-V} > 1$.

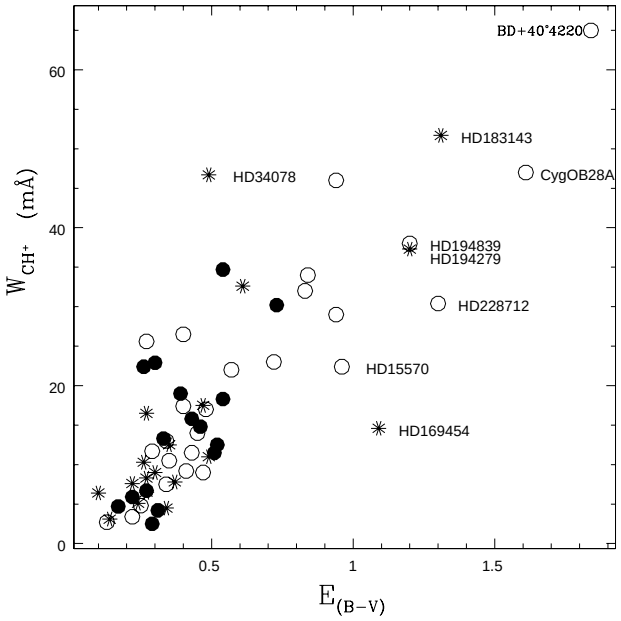

Fig. 2. This plot shows a correlation between CH^+ and E_{B-V} for 70 measured targets with a correlation coefficient of 0.82. Stars which show exceptions are HD34078 and HD169454.

A similar plot for CH^+, measured by using the line at 4232 Å is shown in Fig. 6. In this case the correlation must be considered as very poor, if any (correlation coefficient of 0.11). It is a clear evidence that the chemistry of CH and CH^+ is not the same, and that the conditions required for the respective molecules are quite different. The abundance of CH^+ is apparently not related to the intensity ratio of both major DIBs.

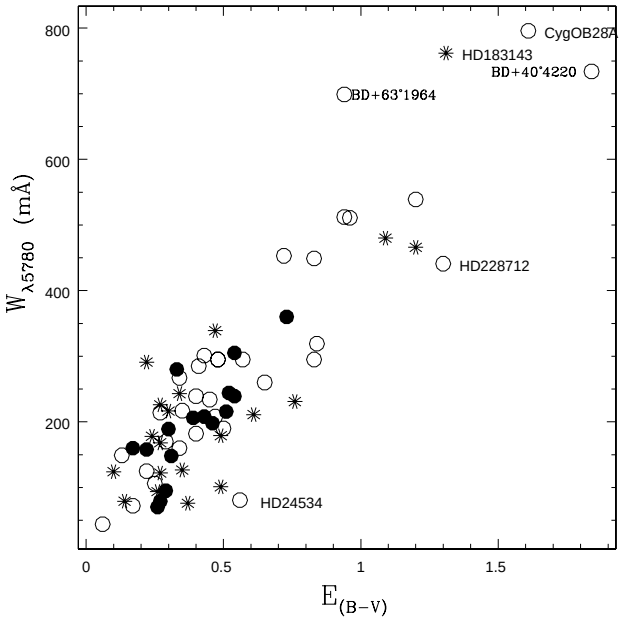

Fig. 3. Fig. 3 displays the relation between the strong, broad DIB at 5780 Å and E_{B-V}. A correlation coefficient of 0.89 can be observed for $\sim$ 70 targets.

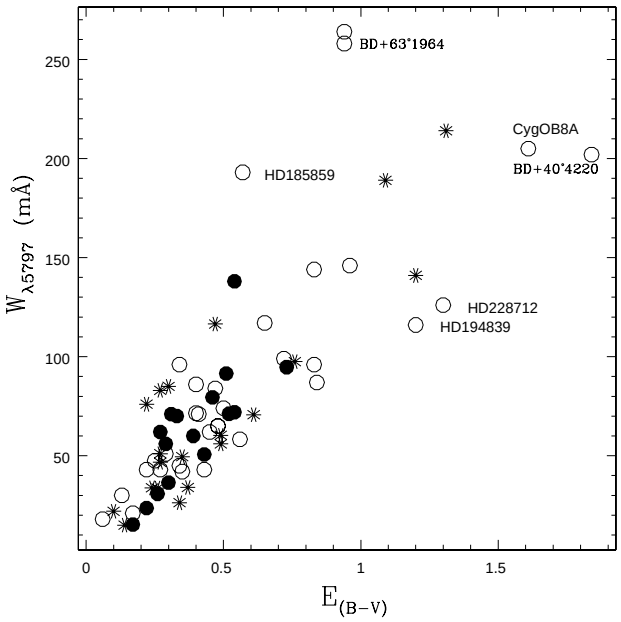

Fig. 4. Fig. 4 displays the correlation between the narrow diffuse band at 5797 Å and E_{B-V}. The correlation coefficient is 0.80 (lower than for the 5780 Å DIB).

4. Discussion

The CH column density is proportional to the H_2 column density (Mattila 1986; Danks et al. 1984). The formation of CH by gas phase reaction involves C^+ and H_2 forming $CH_2{}^+$, which by subsequent dissociative recombination with electrons produces the CH radical. It has been shown that CH correlates with the properties of the far-UV extinction curve (Cardelli 1988; Jenniskens et al. 1992). Thus we may expect CH to be a useful

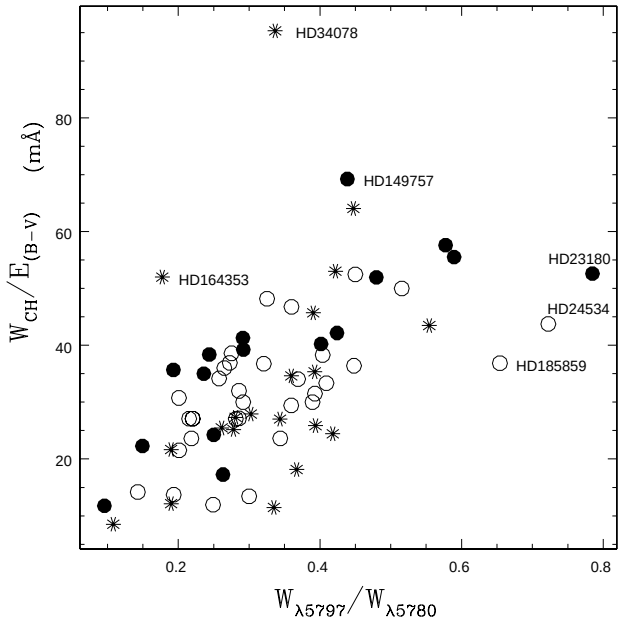

Fig. 5. This figure presents the relation of the ratio CH/E_{B-V} to that of the 5797 to 5780 Å DIBs. Assuming the DIB ratio to be very similar in different measurements in the same target (see tables) we merged the data from different sources to average values avoiding a scatter larger than homogeneous data sets. We measure a correlation coefficient of 0.54 for the parameters CH/E_{B-V} and the 5797/5780 DIB ratio. This confirms that ζ clouds (where λ5797 is favoured) are associated with higher molecular content (CH, H_2).

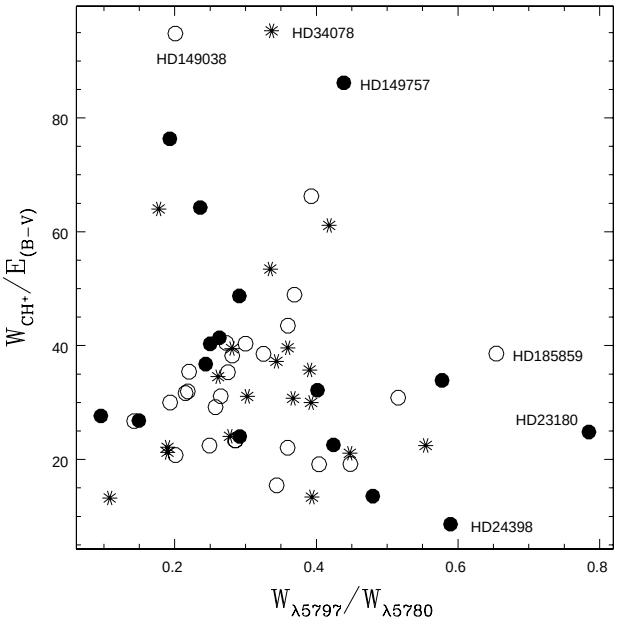

Fig. 6. This figure presents the relation of the ratio CH^+/E_{B-V} to that of the 5797 to 5780 Å DIBs. In this case the correlation of 0.11 is very poor. It is a clear proof that the chemistry and formation conditions of CH and CH^+ are not the same. The abundance of CH^+ is apparently not related to the intensity ratio of both major DIBs.

indicator of the column density of cold-cloud material along a line of sight, since H_2 dominates in cloud cores.

The correlation of CH abundances with reddening for the 70 targets displayed in Fig. 1 shows that CH is less abundant in regions with $E_{B-V} < 0.1$. This is consistent with the formation mechanism of CH, which requires H_2. At very low extinctions, the H_2 abundance is still low despite its rapid self-shielding transition. Between reddening of 0.2 and 0.6 mag the CH molecule shows a good correlation for the observed targets. At higher values of E_{B-V} the CH abundance starts to level off, probably due to the decreasing C^+ abundance (van Dishoeck et al. 1989). In this regime we know little about H_2 abundances because the *Copernicus* satellite was not sufficiently sensitive - but within a few months we expect to have data on H_2 abundances in such clouds, from *FUSE*. At that time we will be able to further explore the relationships among CH, H_2, UV extinction, and the DIBs.

The close connection between CH and other diffuse cloud parameters such as the UV extinction curve and especially R_V, along with the correlation presented here between the DIB ratio 5797/5780 and CH, suggest that these DIBs and CH arise in related physical regions inside diffuse clouds. However, the place of favoured formation of these different species inside the clouds will vary according to the photoionization and chemical reaction balance, and will depend on the UV penetration in the cloud, determined by the local dust VUV extinction curve. This may prove to be significant in the quest to find the DIB carriers.

Interstellar CH^+ abundances are still far from understood. The formation and behavior of this molecular ion have presented a longstanding problem in astrochemistry, as there is no quiescent exothermic reaction by which it can form. Further, CH^+ is rapidly destroyed by reaction with H and $H_2{}^+$, and the observed high CH^+ abundances in the interstellar medium are not compatible with models of quiescent clouds. CH^+ may be formed in shocks or other energetic sources which enable the endothermic reaction $C^+ + H_2 \longrightarrow CH^+ + H$ to occur. A recent model suggests that dissipation of interstellar cloud turbulence may explain CH^+ formation (Gredel 1997). In any event, it appears likely that CH^+ forms outside of the cores of diffuse and translucent clouds; i.e. either in cloud boundary regions or intercloud environments. High-dispersion spectra support this suggestion, as there is often a distinct velocity separation between CH^+ and neutral diatomics such as CH and CN, indicating that CH^+ forms somewhere else along the line of sight (Allen 1994). In view of the correlation we find between the DIB ratio and CH, it would have been very surprising to find any strong relationship between the DIBs and CH^+.

It has been previously suggested (Krełowski et al. 1987) that the far-UV rise of extinction curve may be related to the formation of the widely-studied 4430 DIB. The ratio of this band to E_{B-V} was found to be related to the ratio of the 5797 and 5780 DIBs as well as to a parameter characterizing the far-UV rise of the extinction curve. This, along with earlier work on the behavior of DIBs in dark clouds (e.g. Wampler 1966; Snow & Cohen 1974), suggests that the 4430 Å DIB is formed by a similar class of carriers as the 5797 and 5780 Å DIB, a

conclusion supported by the recent CCD-based survey of λ4430 by Snow, Boyd, & Massey (1999).

5. Conclusions

Several conclusions may be inferred from the above mentioned observational results:

- CH requires the initial radiative association reaction $C^+ + H_2 \longrightarrow CH_2{}^+ + h\nu$. At very low extinction the H_2 abundance is too low to produce efficiently CH;
- the absorption spectra (extinction, molecular features, DIBs) of diffuse and translucent interstellar clouds show significant differences from one object to another. The differences are most easily observable in spectra of nearby stars, where strong contrasts in extinction laws are observed (i.e.; ζOph vs. σSco clouds). This point has been made several times before, as noted in Sect. 1;
- the intensity ratio of the 5797 and 5780 Å DIBs is related to the abundance of cold-cloud molecular species such as CH (and by inference H_2), as well as to the properties of the interstellar dust, especially as seen in far-UV extinction curves;
- the correlation between the 5797/5780 Å DIB ratio and CH/E_{B-V} indicate a balance between the carriers of these two DIBs, with the λ5797 carrier being favoured in environments with higher molecular gas content. This correlation is in qualitative agreement with the photoionization balance of the λ5797 and λ5780 carriers as described by Sonnentrucker et al. (1997), where their contribution (EW/E_{B-V}) peaks at E_{B-V} of 0.25 and 0.17 respectively in single clouds, while the CH relative abundance still grows from E_{B-V}=0.1 to 0.8;
- the correlation between the 5797/5780 ratio and the CH/E_{B-V} abundance indicates that the carriers of these two DIBs thrive in the same regions as CH and H_2 (i.e. diffuse and translucent cloud cores);
- the extremely poor correlation between the DIB ratio and the abundance of CH^+/E_{B-V} shows that the DIBs are not formed in the same regions where CH^+ is formed;
- the intensity ratio of 5797 and 5780 diffuse bands seems to be a very useful parameter indicating the general properties of molecules in diffuse and translucent interstellar clouds.

Acknowledgements. We thank the staff of SAO, OHP, CFHT, ESO, OHP and MCD for support during the observations. This paper has been supported by the II US–Poland Maria Skłodowska–Curie Joint Fund under the grant MEN/NSF–94–196. PE is a recipient of an APART fellowship of the Austrian Academy of Sciences.

References

Adams W.S., 1949, ApJ 109, 354
Allen M.M., 1994, ApJ 424, 754
Baudrand J., Böhm T., 1992, A&A 259, 711
Baranne A., Queloz D., Mayor M., et al., 1996, A&AS 119, 373
Cami J., Sonnentrucker P., Ehrenfreund P., Foing B.H., 1997, A&A 326, 822
Cardelli J.A. 1988, ApJ 335, 177
Crane P., Lambert D.L., Sheffer Y., 1995, A&AS 99, 107
Crawford I.A., Barlow M.J., Diego F., Spyromillo J., 1994, MNRAS 266, 903
Crawford I.A., 1989, MNRAS 241, 575
Crawford I.A., 1997, MNRAS 290, 41
Danks A.C., Federman S.R., Lambert D.L., 1984, A&A 130, 62
Ehrenfreund P., Foing B.H., 1996, A&A 307, L25
Ehrenfreund P., Cami J., Dartois, E., Foing B.H., 1997, A&A 318, L28
Federman S.R., Strom C.J., Lambert D.L., et al., 1994, ApJ 424, 772
Foing B.H., Ehrenfreund P., 1994, Nat 369, 296
Foing B.H., Ehrenfreund P., 1997, A&A 317, L59
Galazutdinov G.A., 1992, Spets. Astrof. Obs. No. 92, preprint
Gredel R., van Dishoeck E.F., Black J.H., 1991, A&A 251, 625
Gredel R., 1997, A&A 320, 929
Heger M.L., 1922, Lick Obs. Bull. 10, 146
Herbig G.H., Soderblom, 1982, ApJ 252, 610
Herbig G.H., 1993, ApJ 407, 142
Herbig G.H., 1995, ARA&A 33, 19
Hobbs L.M., 1978, ApJS 38, 129
Jenniskens P., Ehrenfreund P., Désert X., 1992, A&A 265, L1
Jenniskens P., Désert X., 1994, A&AS 160, 39
Josafatsson K., Snow T.P., 1987, ApJ 319, 436
Kerr T.H., Hibbins R.E., Fossey S.J., Miles J.R., Sarre P.J., 1998, ApJ 495, 941
Krełowski J., Walker G.A.H., 1987, ApJ 312, 860
Krełowski J., Walker G.A.H., Grieve G.R., Hill G.M., 1987, ApJ 316, 449
Krełowski J., Westerlund B.E., 1988, A&A 190, 339
Krełowski J., Snow T.P., Seab C.G., Papaj J., 1992, MNRAS 258, 693
Krełowski J., Sneden C., 1993a, PASP 105, 1141
Krełowski J., Sneden C., 1993b, In: Cutri R., Latter W. (eds.) The First conference of galactic cirrus and diffuse interstellar clouds. ASP 58, 12
Krełowski J., Sneden C., Hiltgen D., 1995, Planetary Space Sci. 43, 1195
Krełowski J., Schmidt M., 1997, ApJ 477, 209
Krelowski J., Galazutdinov G.A., Musaev F.A., 1998, ApJ 493, 217
Mattila R., 1986, A&A 160, 157
Munch G., 1957, ApJ 125, 42
Salama F., Bakes E.L.O., Allamandola L.J., Tielens A.G.G.M., 1996, ApJ 458, 621
Sarre P.J., Miles J.R., Kerr T.H., et al., 1995, MNRAS 277, L41
Seab C.G., Snow T.P., 1995, ApJ 443, 698
Snow T.P., 1997, In: Pendleton Y.J., Tielens A.G.G.M. (eds.) From Stardust to Planetesimals. ASP Conf. Ser. 122, Astronomical Society of the Pacific, San Francisco, p. 147
Snow T.P., Cohen J.G., 1974, ApJ 194, 313
Snow T.P., Bakes E.L.O., Buss R.H., Seab C.G., 1995, A&A 296, L37
Snow T.P., Boyd J., Massey P., 1999, PASP, submitted
Sonnentrucker P., Cami J., Ehrenfreund P., Foing B.H., 1997, A&A 327, 1215
Ó Tuairisg S., Cami J., Foing B.H., Sonnentrucker P., Ehrenfreund P., 1999, submitted to A&AS
Tulej M., Kirkwood D.A., Pachov M., Maier J.P., 1998, ApJ 506, L69
van Dishoeck E.F., Black J.H., 1989, ApJ 340, 273
Wampler E.J., 1966, ApJ 144, 921